

# A Rapid Subcortical Amygdala Route for Faces Irrespective of Spatial Frequency and Emotion

Jessica McFadyen<sup>\*1,2,6</sup>, Martial Mermillod<sup>4,5</sup>, Jason B. Mattingley<sup>1,3,6</sup>, Veronika Halász<sup>1</sup>, and Marta I. Garrido<sup>1,2,6</sup>

<sup>1</sup> Queensland Brain Institute, University of Queensland, St Lucia, QLD, Australia

<sup>2</sup> Centre for Advanced Imaging, University of Queensland, St Lucia, QLD, Australia

<sup>3</sup> School of Psychology, University of Queensland, St Lucia, QLD, Australia

<sup>4</sup> Université Grenoble Alpes, LPNC, F-38000 Grenoble, France & CNRS, LPNC, F-38000 Grenoble, France

<sup>5</sup> Institut Universitaire de France, Paris, France

<sup>6</sup> Australian Research Council of Excellence for Integrative Brain Function, Australia

\* corresponding author: [j.mcfadyen@uq.edu.au](mailto:j.mcfadyen@uq.edu.au)

## ABSTRACT

There is significant controversy over the anatomical existence and potential function of a direct subcortical visual pathway to the amygdala. It is thought that this pathway rapidly transmits low spatial frequency information to the amygdala independently of the cortex and yet this function has never been causally determined. In this study, neural activity was measured using magnetoencephalography (MEG) while participants discriminated the gender of neutral and fearful faces filtered for low or high spatial frequencies. Dynamic causal modelling (DCM) revealed that the most likely underlying neural network consisted of a subcortical pulvino-amygdala connection that was not modulated by spatial frequency or emotion and a cortico-amygdala connection that conveyed predominantly high spatial frequencies. Crucially, data-driven neural simulations demonstrated a clear temporal advantage of the subcortical route (70ms) over the cortical route (155ms) in influencing amygdala activity. Thus, our findings support the existence of a rapid functional subcortical pathway that is unselective of the spatial frequency or emotional content of faces.

## Introduction

The ability to rapidly detect external threats is essential to the survival of all species<sup>1</sup>. The amygdala has long been known to be involved in processing ambiguous and biologically-relevant stimuli<sup>2</sup> but there is considerable controversy over how quickly the amygdala engages in visual processing<sup>2</sup>. One proposition born from converging human and animal evidence is that there is a short and direct colliculo-pulvino pathway to the amygdala<sup>3</sup>. This so-called ‘low road’ is thought to transmit coarse visual information more rapidly than alternative ‘high roads’, which are thought to transmit fine-grained details via the visual cortex<sup>4</sup>. This multi-pathway proposition has sparked debate within the literature over the possible function and even the very existence of the low road<sup>5-8</sup>. The amygdala plays an important modulatory role in coordinating responses to biologically-relevant stimuli<sup>9,10</sup> and in unconscious affective processing<sup>3,11</sup>. As such, it is essential that we understand the potential influence that a subcortical pathway might have over the earliest stages of numerous, cascading processes emanating from the amygdala.

Several studies have supported the anatomical existence of a subcortical pathway to the amygdala, as shown by diffusion imaging<sup>12,13</sup>, computational modelling<sup>14,15</sup>, and neuroanatomical tracing<sup>16,17</sup>. The estimated synaptic integration time of this relatively shorter pathway (estimated length: 58mm, estimated latency: 80-90ms)

41 compared with the cortical visual stream (estimated length: 164mm, estimated latency: 145-170ms) suggests that  
42 the amygdala receives subcortical information faster than cortical information<sup>18</sup>.

43 This rapid subcortical pathway is thought to facilitate early processing of coarse visual information, such as low  
44 spatial frequency content, conveying the general “gist” of a visual scene to the amygdala<sup>19</sup>. Initial support for this  
45 notion came from a seminal functional magnetic resonance imaging (fMRI) study that found greater blood-  
46 oxygen-level-dependent (BOLD) signal in the superior colliculus, pulvinar, and amygdala to low spatial frequency  
47 fearful faces, while the extrastriate visual cortex showed greater BOLD signal for high spatial frequency faces<sup>20</sup>.  
48 These findings have recently been validated at the electrophysiological level, where fearful faces were found to  
49 evoke early activity (75ms post-stimulus onset) in the lateral amygdala but only when the faces were filtered for  
50 low spatial frequency<sup>21</sup>.

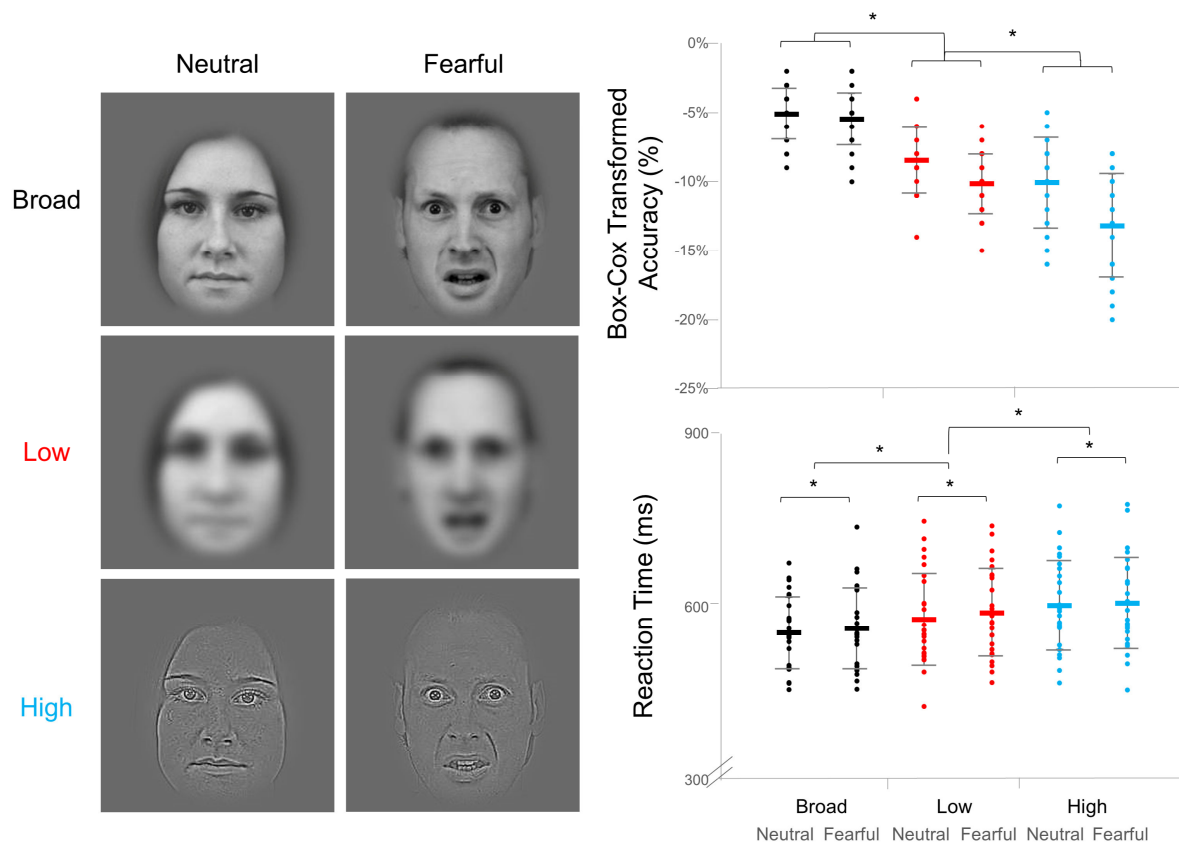
51 These studies do not address the critical element of causality, which is essential for investigating the influence of  
52 the subcortical route. While there is evidence that the neurons of the human superior colliculus are  
53 magnocellular<sup>22</sup>, little is known about the spatial frequency sensitivity of the human pulvinar<sup>23</sup>, although there is  
54 evidence that the pulvinar may be responsive to affective content<sup>24,25</sup>. Therefore, amygdala activation to low  
55 spatial frequency images should not be interpreted as being driven solely by a subcortical pathway. The fragility  
56 of this relationship is demonstrated by the often mixed findings as to whether low spatial frequency emotional  
57 stimuli are processed more rapidly<sup>26</sup>.

58 The aim of this study was to evaluate the causal direction of information flow along the cortical and subcortical  
59 pathways to the amygdala. Neural activity was measured with high temporal resolution using  
60 magnetoencephalography (MEG) while participants made gender judgements on faces filtered for different spatial  
61 frequencies. Dynamic causal modelling was then applied to these data to infer the direction of information  
62 transmission within hypothesised neural networks, using biophysically informed methods and Bayesian model  
63 comparison<sup>27</sup>. The hypothesised networks consisted of four increasingly complex models: 1) cortical connection  
64 from lateral geniculate nucleus to primary visual cortex (V1) to amygdala, 2) cortical connection plus a subcortical  
65 connection from pulvinar to amygdala, 3) cortical connection plus a medial connection from pulvinar to V1 to  
66 amygdala, and 4) cortical, subcortical, and medial connections. The medial connection was included to account  
67 for the possibility that the pulvinar influences amygdala activity indirectly via cortical sources<sup>9</sup>. After determining  
68 the most likely underlying neural architecture made up of a combination of these different processing streams,  
69 hypotheses were tested for the types of spatial frequency content propagated along each connection. Using this  
70 approach, we aimed to determine whether the subcortical pathway, if active, is modulated primarily by low spatial  
71 frequency images of biologically-relevant stimuli (i.e. neutral and fearful faces).

## 72 **Results**

### 73 **Gender Discrimination Performance**

74 Participants were instructed to report the gender of faces as quickly and accurately as possible. Faces were either  
75 unfiltered (i.e. broad spatial frequency) or filtered to contain only low or high spatial frequencies and either had a  
76 neutral or fearful expression. Outlier trials (i.e. trials where reaction time was more than 3 standard deviations  
77 above or below the mean for that participant) were removed from statistical analyses ( $M = 7.73\%$ ,  $SD = 4.24\%$  of  
78 trials). Shapiro-Wilk tests revealed that the accuracy data was negatively skewed and thus Box-Cox  
79 transformations were conducted to satisfy conditions of normality. Hence, 2 (emotion) x 2 (spatial frequency)  
80 repeated-measures ANOVAs were conducted separately for reaction time (correct responses only) and the Box-  
81 Cox-transformed accuracy data. Greenhouse-Geisser values were used where appropriate and Bonferroni  
82 adjustments were made to correct for multiple comparisons. All reported statistics are significant at  $p < .05$ .



83

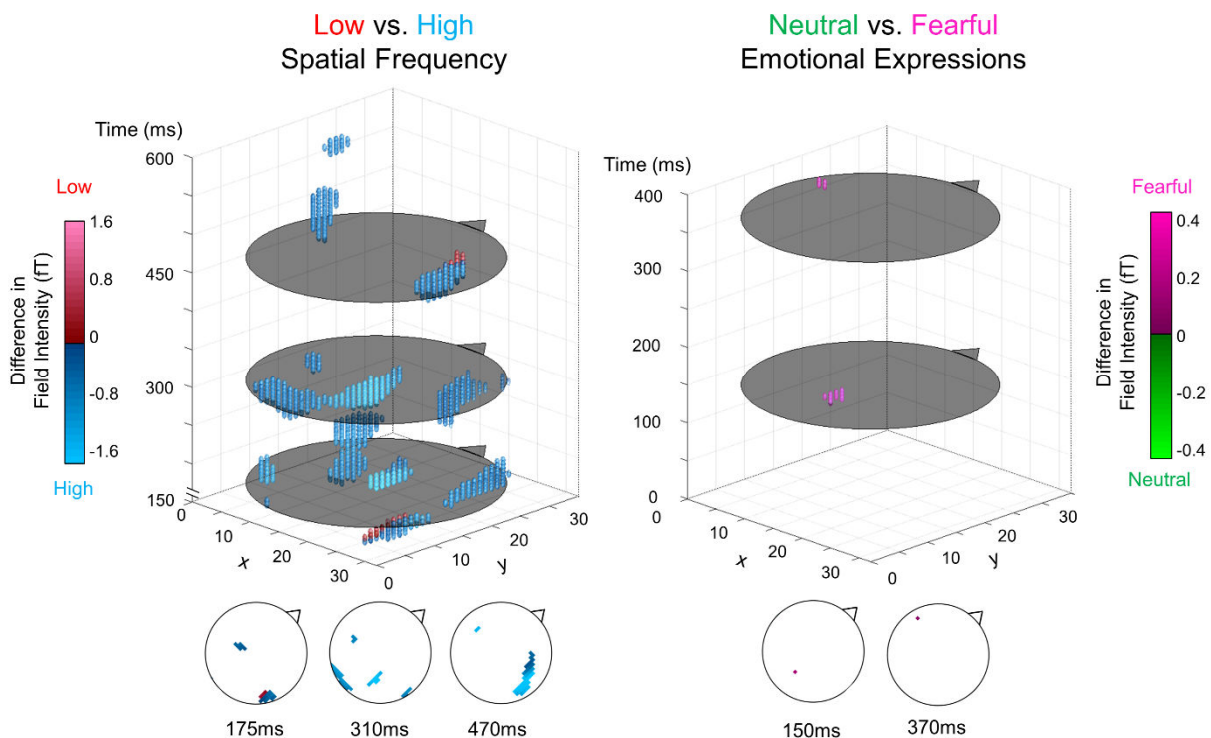
84 **Figure 1: Experimental design and behavioural data.** (Left) Examples of the face stimuli used in the  
 85 experiment. The columns depict the Neutral and Fearful Emotion conditions and the rows depict the three spatial  
 86 frequency conditions: Broad, Low, and High. (Right) Dot plots of each participant's score for accuracy (top) and  
 87 reaction time (bottom) in the gender judgement task. The accuracy data was Box-Cox transformed to satisfy  
 88 conditions of normality. Black indicates Broad spatial frequency, red indicates Low, and blue indicates High. Each  
 89 spatial frequency column contains a pair, where the left series represents Neutral expressions and the right  
 90 series represents Fearful expressions. Standard error bars shown. \*  $p < .05$

91 Higher accuracy ( $F(1, 32) = 108.29, p = 6.65 \times 10^{-13}$ ) and faster reaction time ( $F(2, 41) = 47.14, p = 2.30 \times 10^{-10}$ )  
 92 were found for Broad spatial frequency faces (-5.30%, 559ms) than for Low (-9.29%, 585ms) spatial frequency  
 93 faces and likewise for Low relative to High spatial frequency faces (-11.65%, 605ms). Significantly higher  
 94 accuracy ( $F(1, 25) = 116.46, p = 6.74 \times 10^{-11}$ ) and faster reaction time ( $F(1, 25) = 12.24, p = .002$ ) were found  
 95 overall for Neutral faces (-7.89%, 579ms), compared with Fearful faces (-9.60%, 587ms). An interaction was  
 96 found in accuracy scores, such that the emotion effect was only present for Low and High spatial frequencies  
 97 ( $F(2, 43) = 24.89, p = 2.33 \times 10^{-7}$ ). Thus, gender discrimination was impaired more by the removal of low than  
 98 high spatial frequencies. Furthermore, fearful faces slowed reaction times overall. Accuracy, however, was  
 99 impaired by fearful expressions only when images were filtered for low and high spatial frequency.

100 Although gender discrimination performance has previously been thought of as equivalent between low and high  
 101 spatial frequency faces<sup>20,28,29</sup>, our results support other studies that have found an advantage of low over high  
 102 spatial frequency information<sup>30-34</sup>. Interestingly, few of these studies report an influence of emotional expression  
 103 on performance<sup>35</sup>, which contrasts with our findings. The average luminance and root-mean-square contrast did  
 104 not differ significantly between emotion conditions, as determined by separate 2 (emotion) x 3 (spatial frequency)  
 105 repeated-measures ANOVAs, and so the difference was not likely due to low-level perceptual confounds. It is  
 106 possible that fearful faces impaired performance because participants were instructed to respond as quickly (and  
 107 as accurately) as possible, whereas such a time pressure may have been absent in previous studies.

## 108 Spatiotemporal Analysis of MEG Sensor Data

109 Statistical parametric mapping was applied to neural data collected from 204 planar gradiometers. This sensor  
110 activity (field intensity) was converted into 3D maps of space ( $x$  and  $y$  mm<sup>2</sup>) and time (0-600ms, 5ms resolution).  
111 A 2 (emotion) x 3 (spatial frequency) within-subjects design was then modelled in a mass univariate analysis,  
112 correcting for multiple comparisons using Random Field Theory, as is typically performed in standard general  
113 linear model (GLM) analysis of fMRI data. The resultant statistical parametric maps were then compared between  
114 participants in a series of planned comparisons: 1) Low vs. High spatial frequency, 2) Neutral vs. Fearful Emotion,  
115 and 3) Interaction between Low and High spatial frequency and emotion. Broad spatial frequency was also used  
116 as an ecological control for Low and High spatial frequency in a set of two comparisons: Broad vs. Low and  
117 Broad vs. High (see **Supplementary Information** for a visualization of these results). All the following results  
118 for each comparison are  $p < .05$ , family-wise-error-corrected.



119

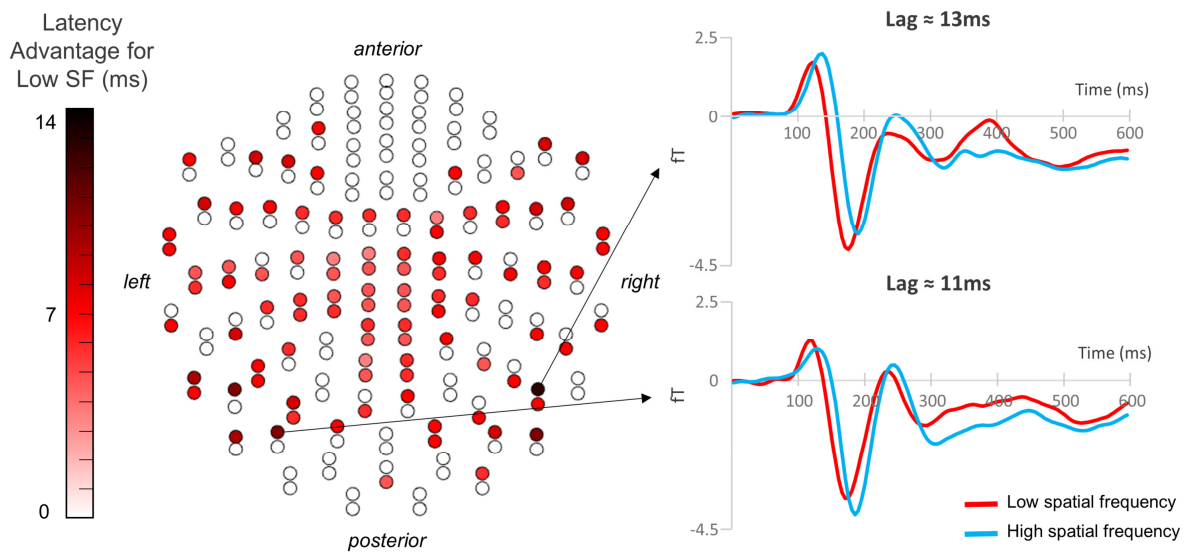
120 **Figure 2: Statistical parametric maps of sensor data.** A 3D representation of significant voxels across space  
121 and time. The flat grey circles in the 3D plot represent time-points of interest (for graphical purposes) which are  
122 each displayed as traditional scalp plots along the bottom of the figure (triangle/nose indicates faced direction). For  
123 Low vs. High spatial frequency (left), blue and red spheres indicate voxels that had significantly greater absolute  
124 field intensity for High and Low spatial frequency faces, respectively. Similarly, for Neutral vs. Fearful on the right,  
125 pink and green indicate greater absolute field intensity for Fearful and Neutral expressions, respectively. All points  
126 are significant at  $p < .05$ , family-wise error corrected.

127 Significant differences in field intensity were found between Low and High spatial frequency across occipital,  
128 temporal, and central areas, spanning a time-window of 160-585ms (set-level  $F(2,25) = 38.86$ ,  $p = 1.61 \times 10^{-6}$ ;  
129 **Fig. 2**). Greater absolute field intensity for Low spatial frequency was found at the earliest significant time point  
130 (160ms) over right occipito-temporal areas and later on at 460 and 465ms over right temporal areas. All remaining  
131 clusters of significant activity showed greater field intensity for High than Low spatial frequency faces. These  
132 clusters were found at various time-points between 170 and 585ms, located bilaterally and centrally over occipital  
133 and parietal areas. Thus, we found distinct early (160ms) and late (460ms) components of Low spatial frequency  
134 processing despite overwhelmingly greater activity for High spatial frequency overall (170-585ms). Previous  
135 studies have also reported greater neural activity for Low than High spatial frequency images at approximately  
136 160ms<sup>31,34,36</sup>. Moreover, similar findings have been reported for overall greater amplitude for High compared with  
137 Low spatial frequency faces<sup>35,37,38</sup>, with some studies reporting an earlier modulation than presented here (i.e. the  
138 M100 compared with the M170)<sup>37,38</sup>. This discrepancy may be due to differences in analysis technique, such that

139 statistics on specific electrodes and time-windows are more specific (but also biased) compared with our more  
140 conservative and unbiased spatiotemporal analysis, where corrections for multiple comparisons are made across  
141 the entire sensor space and all time-points.

142 Activity elicited by Fearful faces was significantly greater than by Neutral faces at two distinct clusters: an  
143 occipital peak at 150ms and a left temporal peak at 370ms (set-level  $F(1,25) = 38.48$ ,  $p = 1.73 \times 10^{-6}$ ), indicating  
144 typical early and late emotion effects as reported in the literature<sup>39</sup>. This effect did not, however, interact  
145 significantly with spatial frequency. Thus, although Low spatial frequency processing was indeed found to be  
146 faster overall, this did not result in enhanced processing of fearful faces. Hence, our findings do not support an  
147 automatic prioritisation of Low spatial frequency fear processing, which is in line with the findings of a recent  
148 meta-analysis<sup>26</sup>.

### 149 **Assessing Neural Latency with Cross-Correlation**



150

151 **Figure 3: Latency advantage for low spatial frequency faces.** (Left) A sensor map displaying 204 planar  
152 gradiometers, where red indicates a sensor that showed a significant time difference between Low and High spatial  
153 frequency, such that darker red indicates an earlier neural effect of Low compared with High spatial frequency  
154 faces. (Right) Activity at two example sensors that showed the greatest time difference.

155 In the spatiotemporal analysis, the earliest significant difference between spatial frequency activation was found  
156 at 160ms, where field intensity was greater for Low than High spatial frequency, followed by significantly greater  
157 activity for High than Low at 170ms onwards. To determine whether this apparent temporal difference was  
158 significant, cross-correlation analyses were performed. This approach assumes that two paired waveforms (i.e.  
159 Low and High spatial frequency ERFs at each sensor) are highly correlated, which was indeed the case in this  
160 dataset (average  $R^2$  across channels and subjects = 82.79%). Thus, we computed the relative lag between these  
161 waveforms at each of the 204 sensors. This resulted in 96 (47.06%) of sensors with a significant lag (Bonferroni-  
162 corrected,  $p < 2.45 \times 10^{-4}$ ) between Low and High spatial frequency faces, where all 204 sensors demonstrated an  
163 earlier effect of Low spatial frequency ( $M = 7.13\text{ms}$ ,  $SD = 2.19\text{ms}$ ; **Fig. 3**). This finding is supported by similar  
164 studies showing earlier M170 latencies for Low compared with High spatial frequency image processing<sup>34,35</sup>.  
165 Therefore, there appears to be a significant temporal disadvantage for High compared with Low spatial frequency  
166 faces, such that the waveform as a whole (which encompasses multiple face processing components like the M100  
167 and M170) is shifted later in time.

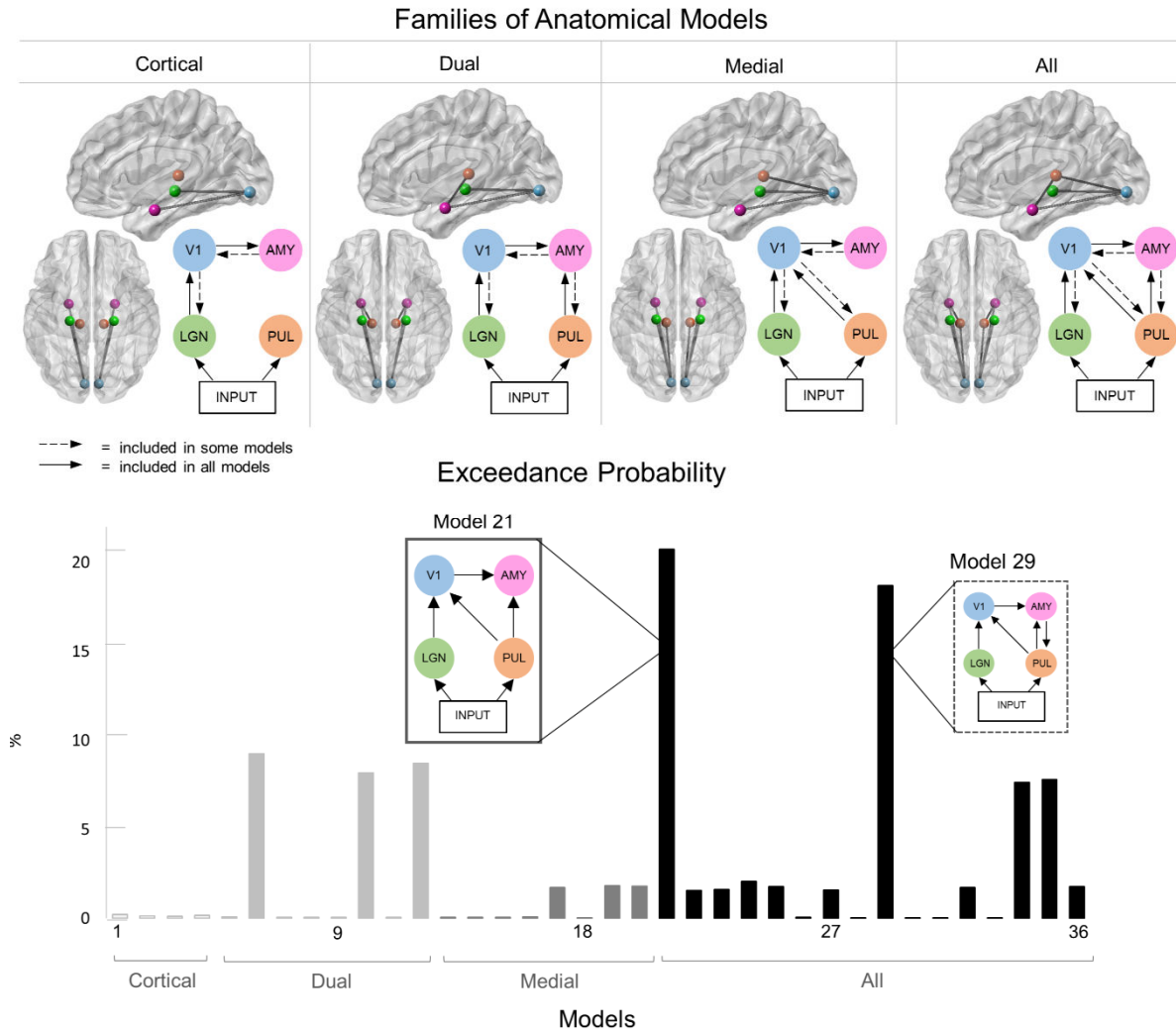
### 168 **Dynamic Causal Modelling of Neural Networks**

169 Dynamic causal modelling is a biophysically informed method of comparing the likelihood of hypothetical neural  
170 networks that underlie a given dataset, compromising between model accuracy and complexity<sup>27</sup>. This technique  
171 was used in two stages: an *anatomical* stage, where we compared the likelihood that cortical, medial, and  
172 subcortical connections were recruited across all conditions, and a *functional* stage, where we took the winning



173 model from the previous stage and compared the likelihood that connections were modulated by spatial frequency  
 174 and/or emotion.

175 Sources were modelled using equivalent current dipoles based on validated functional coordinates from previous  
 176 literature (MNI coordinates: LGN – left [-22, -22, -6], right [22 -22 -6]; V1 – left [-7 -85 -7], right [7 -85 -7];  
 177 pulvinar – left [-12 -25 7], right [12 -25 7]; amygdala – left [-23 -5 -22], right [23 -5 -22])<sup>14</sup>. Input was modelled  
 178 as entering the LGN and pulvinar and only the first 300ms of activity post-stimulus onset was modelled so as to  
 179 capture early visual processing, specifically.

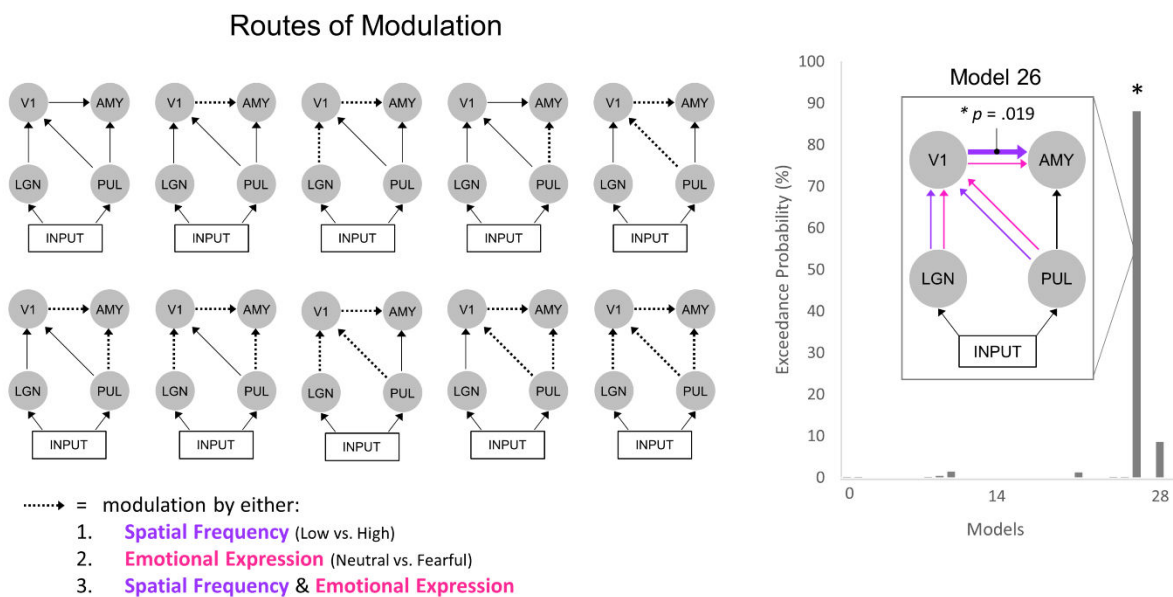


180

181 **Figure 4: Selection of families of anatomical models.** (Top) Four families of anatomical models were tested.  
 182 Green nodes represent the LGN, blue the primary visual cortex (V1), pink the amygdala (AMY), and orange the  
 183 pulvinar (PUL). The 3D brain images (sagittal and axial views) are shown. Note that all models consisted of  
 184 separate left and right hemispheres. (Bottom) The exceedance probability of each model, grouped into the four  
 185 families (light grey for Cortical, grey for Subcortical, dark grey for Medial, and black for All). Model 21, which had  
 186 the highest probability, is shown in the left break-out box, while the next most probable model, Model 29, is  
 187 shown in the right break-out box.

188 In the anatomical stage, four families of models were constructed (**Fig. 4**). Each family consisted of models for  
 189 each possible combination of forward and backward connections, resulting in four models for the Cortical family,  
 190 eight models for Dual, eight models for Medial, and sixteen models for All. Each model contained nodes for the  
 191 left and right hemispheres but cross-hemisphere connections (e.g. from the left amygdala to the right amygdala)  
 192 were not modelled.

193 Random effects Bayesian Model Selection was conducted on all models grouped into families. The greatest  
 194 exceedance probability was found for the All family (59.61%) compared with the Dual (23.69%), Medial  
 195 (13.29%), and Cortical (3.40%) families. Therefore, it is clear that the inclusion of the subcortical route (i.e. the  
 196 All and Dual families) vastly increased model likelihood. Within the winning All family, two models had  
 197 comparably higher exceedance probability than the other fourteen: Model 21 (20.72%) and Model 29 (18.69%).  
 198 Model 21 was the simplest in the family of models, containing only forward connections, whereas Model 29 was  
 199 only incrementally more complex due to the addition of a backward connection between the amygdala and  
 200 pulvinar. Since previous research has established that backward connections contribute more to a model's  
 201 explanatory power as peristimulus time increases<sup>40</sup>, we speculate that the below-chance difference between these  
 202 two models (chance being 100% divided by the number of models in the space, giving 2.78%) may be because  
 203 the backward connection's effect only occurred in the latter part of the 0-300ms time-window. Applying Occam's  
 204 razor, we selected Model 21 as the most parsimonious explanation for our data because this model had the fewest  
 205 connections and also the greatest exceedance probability. Hence, the anatomical foundation for the following  
 206 series of functional models consisted of the well-known cortical stream, the controversial subcortical pathway,  
 207 and the hypothesised medial connection between the pulvinar and the visual cortex.



208

209 **Figure 5: Routes of modulation by emotion and spatial frequency.** (Left) Each diagram depicts a plausible  
 210 route of modulation, where the dotted arrows indicate potential modulation by spatial frequency, emotion, or both.  
 211 Note that the first model in the upper left is the Null model with no modulated connections. The other nine models  
 212 were each uniquely modulated. (Right) The exceedance probability, determined via Bayesian Model Selection,  
 213 for all 29 models. The model shown in the break-out box is the winning model (Model 26), where all connections  
 214 were modulated by spatial frequency and emotion except the subcortical route. Classical t-tests revealed that  
 215 only the parameter estimates for the cortical connection were significantly greater than zero ( $p = .019$ ).

216 The functional stage was designed to determine the likelihood of different routes of modulation by spatial  
 217 frequency, emotion, or both, using a between-trial effects approach (i.e. differences between Low and High spatial  
 218 frequency or between Neutral and Fearful emotional expressions)<sup>41</sup>. First, we determined the possible paths along  
 219 which visual information may be modulated (four possibilities: V1-AMY, LGN-V1-AMY, PUL-AMY, PUL-V1-  
 220 AMY). These modulatory pathways were then combined in every possible way, resulting in nine models each for  
 221 modulation by spatial frequency, emotion, or both (**Fig. 5**). Thus, the entire model space consisted of 28 models,  
 222 including a null model precluding any modulation.

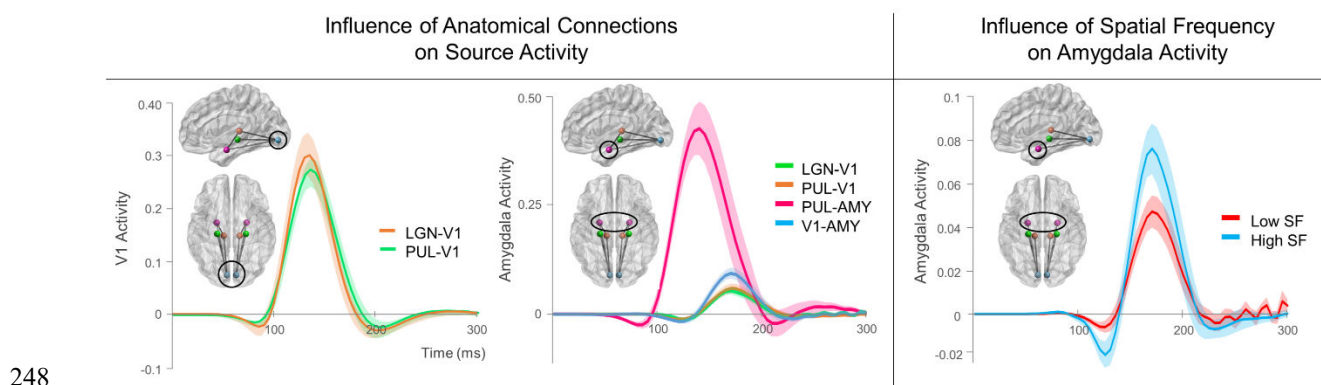
223 Random effects Bayesian Model Selection revealed that Model 26 had the greatest exceedance probability  
 224 (88.04%), demonstrating that all pathways except the subcortical pathway were likely modulated by both spatial  
 225 frequency and emotion within the given dataset. To infer the generalizability of this neural network to the  
 226 population, classical one-sample *t* tests were conducted on individual parameter (i.e. connection) estimates. After

227 Bonferroni correction for multiple comparisons, only the modulation of the cortical connection from primary  
228 visual cortex to amygdala was significantly greater than zero ( $p = .019$ ).

## 229 Sensitivity Analysis

230 Having found a clear winning model for both the underlying neural architecture and the likely modulation of  
231 parameters by spatial frequency and emotion, we investigated the direction of information flow in the network  
232 (i.e. was V1-amygdala activity greater for high or low spatial frequency?) and also the timing of flow within the  
233 network (i.e. did the subcortical pathway perturb amygdala activity earlier than the cortical pathway?) To do this,  
234 we employed sensitivity analysis, which uses simulated data generated by an estimated dynamic causal model  
235 inferred from the data. This analysis technique tests the influence of particular parameters within a network by  
236 artificially amplifying coupling strength through stimulation. If the parameter influences the activity at a particular  
237 node in the simulated network, then it should be possible to observe a fluctuation in the simulated activity<sup>42-44</sup>.  
238 Therefore, using a data-driven modelling approach, we were able to make inferences about the influence of the  
239 subcortical, cortical, and medial connections on visual cortex and amygdala source activity.

240 A replica of the winning model was constructed to split the modulatory effects of spatial frequency and emotion at  
241 the cortical and medial streams into Low-Neutral, Low-Fearful, High-Neutral, and High-Fearful (each indicating  
242 spatial frequency and emotional expression, respectively), allowing us to observe interaction effects. Analyses  
243 were conducted separately on the anatomical presence and functional modulation of each connection. Waveforms  
244 of amygdala and V1 source activity were produced for perturbation by each connection type. The entirety of each  
245 of these waveforms was statistically analysed by creating statistical parametric maps (*source activity x time*) and  
246 using Random Field Theory to correct for multiple comparisons across time ( $p < .05$ ), similar to the previous  
247 spatiotemporal analysis.



249 **Figure 6: Sensitivity analysis of connection type on source activity.** Sensitivity Analysis of anatomical  
250 connectivity (left, centre) and modulatory (right) connections. Each wave depicts the simulated perturbation in  
251 source activity by either the presence of a connection, as in the left-hand and centre graphs, or the modulation by  
252 Low or High spatial frequency, as in the right-hand graph.

253 First, we investigated how each anatomical connection influenced V1 and amygdala activity by boosting the  
254 coupling parameters for each connection. V1 source activity was equally influenced by its forward connections  
255 from lateral geniculate nucleus and pulvinar from 110-160ms (**Fig. 6, left**). Changes in amygdala activity, on the  
256 other hand, were significantly greater for the subcortical pathway than for all other connections between 70-90ms  
257 and 110-165ms (**Fig 6., centre**). There was also a significantly greater change in amygdala source activity for the  
258 direct cortical connection from V1 than from the more indirect LGN-V1 (155-190ms) and pulvinar-V1 (165-  
259 180ms) connections.

260 To determine whether these apparent time differences in amygdala perturbation were significant, cross-correlation  
261 was conducted on pairs of the four connections. As expected, the perturbation by the subcortical pathway at 70ms  
262 was significantly earlier than the perturbation by the LGN-V1 (by 33.27ms,  $p = 6.638 \times 10^{-10}$ ), PUL-V1 (by  
263 31.54ms,  $p = 1.956 \times 10^{-12}$ ), and V1-AMY connections (by 32.88ms,  $p = 9.659 \times 10^{-13}$ ), each of which perturbed  
264 activity later at approximately 155ms.



265 A separate sensitivity analysis was conducted on the functional modulation of connections in the winning model.  
266 This first revealed that neither spatial frequency nor emotion modulation influenced V1 source activity through  
267 LGN or pulvinar input pathways. Interestingly, a main effect of Spatial Frequency was found for amygdala source  
268 activity, showing greater perturbation by High than Low spatial frequency during 125-130ms and 165-180ms  
269 (**Fig. 6, right**). Upon observation of each individual connection (i.e. LGN-V1, V1-AMY, and PUL-V1), it appears  
270 that High spatial frequency yielded a greater general effect across connections but that this effect was  
271 predominantly driven by modulation along the cortical V1-AMY connection, which was the only significant  
272 simple effect. This corroborates the significant  $t$  statistic on this parameter found within the winning functional  
273 Model 26.

## 274 **Discussion**

275 We have presented computational evidence supporting the existence of a subcortical route to the amygdala that  
276 facilitates rapid visual information transfer as early as 70ms, irrespective of spatial frequency or emotional content.  
277 Participants viewed low, high, and broad spatial frequency faces exhibiting neutral or fearful expressions.  
278 Performance on a gender discrimination task was better for low than high spatial frequency faces and for neutral  
279 than fearful faces, while neural activity was greater and slower overall for high compared with low and broad  
280 spatial frequency faces. Taken together, this suggests that high spatial frequency faces were more computationally  
281 demanding<sup>45</sup>.

282 Dynamic causal modelling was used to test hypotheses for the most likely structure and function of the neural  
283 network underlying face perception, particularly the rapid processing that occurs within the first 300ms. The  
284 anatomical stage demonstrated that the most likely network consisted of forward-only cortical, subcortical, and  
285 medial connections to the amygdala, providing evidence for the existence of the ‘low road’ to the amygdala that  
286 operates in parallel with the ‘high road’, as shown in previous dynamic causal modelling studies<sup>14,15</sup>. In the  
287 winning model from the functional stage, the cortical and medial pathways were modulated by spatial frequency  
288 and emotion but the subcortical pathway was not, indicating that activity along this pathway was indistinguishable  
289 between conditions. Classical statistics on the parameters themselves revealed that only the spatial frequency  
290 modulation of the cortical connection was consistent across participants and thus generalizable to the population.  
291 Sensitivity analysis on a more detailed replica of the winning model demonstrated that there was significantly  
292 earlier perturbation of amygdala activity by the subcortical route (70ms) than by the cortical or medial pathways  
293 (155ms), regardless of emotion or spatial frequency content.

## 294 **Multiple Parallel Pathways**

295 Our results lend support to anatomical evidence of this pathway<sup>12,17,46</sup>, as well as previous demonstrations of a  
296 functional subcortical route to the amygdala using dynamic causal modelling of MEG data<sup>14,15</sup>. This clearly  
297 illustrates the important causal role of the pulvinar in triggering amygdala activity. Importantly, we also found  
298 evidence for a functional medial connection from the pulvinar to the visual cortex, previously demonstrated in  
299 human and non-human primates<sup>47</sup>. Such a cortico-pulvinar connection has been suggested to mediate the  
300 subcortical pathway, thus rendering it *indirect*<sup>6</sup>. Our results dispute this alternative explanation, as we found the  
301 medial connection to be forward-only and its influence on amygdala activity was estimated to be over 30ms later  
302 than the subcortical route’s influence. Our results therefore support a multiple, parallel processing account of  
303 visual information transfer to the amygdala, within which there exists a rapid subcortical pathway<sup>11</sup>. This adds  
304 significant weight to the prospect that the subcortical route plays a role in unconscious, or pre-attentive, affective  
305 processing by providing a rapid direct pathway to the amygdala that operates independently of the cortex<sup>11,48</sup>.

## 306 **The Subcortical Route is “Blind” to Spatial Frequency**

307 Contrary to our initial hypothesis, the subcortical pathway was modulated neither by spatial frequency nor  
308 emotion. This lack of modulation of the subcortical route by spatial frequency was somewhat unexpected given  
309 previous fMRI findings for increased low spatial frequency activity in the superior colliculus, pulvinar, and  
310 amygdala during emotional face viewing<sup>20</sup>, as well as the widely-held assumption that these subcortical areas  
311 consist of magnocellular neurons<sup>49</sup>. Furthermore, a recent intracranial EEG study by Mendez-Bertolo et al. found  
312 lateral amygdala responses to fearful faces that were specific to low spatial frequencies<sup>21</sup>.

313 One potential explanation for these discrepancies is that our stimuli were matched for both luminance and contrast,  
314 unlike other studies where only luminance was matched<sup>20,21</sup>. The effects of contrast equalisation on spatial  
315 frequency processing are particularly important during early (i.e. < 100ms) visual processing<sup>35</sup>. Supporting this  
316 notion is another intracranial EEG study that used luminance- and contrast-equalized stimuli but did not observe  
317 significant differences between low and high spatial frequency visible faces until 240ms<sup>50</sup>. Thus, teasing apart the  
318 effects of contrast and spatial frequency on subcortical activity may be a promising avenue for future research.

319 Another potential explanation for these apparently conflicting results is that they simply view neural processing  
320 at different scales. A multitude of evidence supports accurate localisation of deep sources in MEG<sup>51,52</sup>, especially  
321 when source reconstruction techniques are used in conjunction with coordinate locations known *a priori* from  
322 fMRI studies employing the same paradigms<sup>14,51,53</sup> such as in the present study. Combining this with a dynamic  
323 causal modelling approach allowed us to consider the likelihood of the broad underlying neural architecture at the  
324 *systems* level and to make inferences on the causal nature of information flow along neural connections. This  
325 critical element of causality was absent in previous fMRI research, leaving open the possibility that the spatial  
326 frequency effects they reported were driven by feedback connections from other neural areas<sup>20</sup>.

327 Electrophysiological approaches, on the other hand, yield highly spatially and temporally specific effects at the  
328 *cellular* level<sup>50,54</sup>. This technique has revealed early spatial-frequency- and emotion-specific effects at the level of  
329 single cell populations within the amygdala<sup>21</sup>. The present findings, however, extend this result by demonstrating  
330 that these cellular differences may be less meaningful when examined at the neural systems level, where we found  
331 a higher likelihood of an *unmodulated* subcortical route than one modulated by spatial frequency or emotion. The  
332 complementary nature of these findings is further supported by the similar latencies found for amygdala  
333 perturbation (approximately 70ms). Hence, while our study provides causal evidence to support the claim that this  
334 early perturbation in the lateral amygdala was driven by the subcortical route<sup>21</sup>, small short-lived differences in  
335 spatial frequency processing may not have been sufficient to be detected (and thus may not be meaningful) at a  
336 broader systems level.

### 337 **Rapid Transmission of both Neutral and Fearful Faces**

338 Emotional expression modulated activity along the medial pulvinar-V1 pathway but not along the subcortical  
339 pathway. This result is consistent with previous dynamic causal modelling studies that also report a lack of  
340 emotional modulation along the subcortical pathway<sup>14,53</sup>. Indeed, we would expect that significant emotional  
341 responses to fearful faces would not be observed until visual information is processed by the amygdala or other  
342 higher-order neural areas<sup>15,55</sup>. This is supported by the latency of the emotion effects we observed at the sensor  
343 level (occurring at approximately 150ms). Some degree of pre-emptive processing in the pulvinar, however, is  
344 supported by previous research on pulvinar response-specificity to faces<sup>24,56</sup> and snakes<sup>24,57,58</sup>. There has been  
345 debate, though, over whether these pulvinar responses are generated independently or are a result of cortical  
346 mediation<sup>6,8</sup>. Our results suggest that the pulvinar is independently capable of some degree of filtering of facial  
347 expressions, as shown by the modulation within the winning model.

### 348 **A Generalised Functional Role of the Subcortical Route**

349 Despite the capability of the pulvinar in filtering both spatial frequency and emotional content, we found the  
350 subcortical route to preclude any such modulation. Therefore, while our findings support a *rapid* subcortical route,  
351 they do not support a *crude* subcortical route, where “crudeness” is operationalised as specificity for low-spatial  
352 frequency information processing. On the contrary, our results provide novel causal evidence for a *generalised*  
353 functional role of the subcortical route, such that neither spatial frequency nor emotional content is filtered.

354 Such a mechanism is intuitive, considering that an organism’s survival is maximised if it can rapidly detect  
355 potential threats using both low *and* high spatial frequencies contained in visual stimuli<sup>59,60</sup>. The so-called  
356 ‘diagnostic approach’ describes flexible prioritisation of spatial frequency processing depending on the task at  
357 hand<sup>61,62</sup>. For example, low spatial frequency information could indicate the presence of a face but high spatial  
358 frequency information could indicate the face’s identity, either of which could be essential for detecting a potential  
359 threat<sup>63</sup>. The amygdala’s purported role as a ‘relevance detector’<sup>64</sup> would suggest that its earliest visual input  
360 would contain all spatial frequencies and all emotional content – hence, the fast subcortical pathway unfiltered for  
361 spatial frequency or emotional content we have demonstrated in the present study. This complements other

362 research on the auditory subcortical route to the amygdala, which was unmodulated by predictable versus  
363 unpredictable sounds<sup>53</sup>.

## 364 **Conclusion**

365 Through the use of causal computational modelling, the present study has identified, for the first time, the causal  
366 functional role of the subcortical route in rapidly transmitting visual information about faces that are unfiltered  
367 for spatial frequency or emotional content. Reframing the subcortical route as playing a generalized role in rapid  
368 emotion processing unifies several opposing theories on why emotional responses to different spatial frequencies  
369 have yielded contradictory findings<sup>6,26</sup>; if the subcortical route transmits all spatial frequencies, as we have shown,  
370 then it may facilitate rapid neural and behavioural responses for both low *and* high spatial frequency stimuli. Thus,  
371 we propose that the supposed “coarseness” of the subcortical route may be better reframed as “unfiltered”. Future  
372 research should investigate whether the subcortical route is in fact capable of filtering spatial frequencies under  
373 certain task demands, as suggested by the diagnostic approach<sup>61–63</sup>, and whether this is influenced by the many  
374 cortical areas connected with the pulvinar, as suggested by previous debates on this topic<sup>6</sup>.

375 This paper makes a significant contribution to the evidence for the functional role of a subcortical route that  
376 operates in parallel with other cortical pathways for emotional visual processing. By understanding precisely what  
377 information is transmitted along this rapid, subcortical pathway and how this is used by the amygdala, we may  
378 better understand the first stages of emotional experience and the potential role subcortical activity plays in  
379 emotional disorders, such as anxiety<sup>65</sup> and autism<sup>66</sup>.

## 380 **Methods**

### 381 **Participants**

382 Twenty-seven people participated in the study, although one was discarded due to being on psychiatric  
383 medication. This left 26 neurologically healthy participants (50% female; 23 right-handed, 3 left-handed) with an  
384 age range from 18 to 32 years ( $M = 22.69$  years,  $SD = 3.87$  years). All participants had normal or corrected-to-  
385 normal vision. Participation in the study was voluntary and all participants were reimbursed AUD\$40 for their  
386 time. Ethical clearance was granted by The University of Queensland Institutional Human Research Ethics  
387 committee.

### 388 **Procedure**

389 All participants were scanned at Swinburne University of Technology in Melbourne, Victoria. After removing all  
390 metal items from the body, participants were seated in the MEG inside a magnetically shielded room. Stimuli  
391 were projected onto a Perspex screen positioned approximately 1.15 meters in front of the participant (viewing  
392 angle  $\approx 22.81^\circ$ ). Participants held a MEG-compatible 2-response button box with their dominant hand with the  
393 index and middle finger resting on the two buttons (akin to a computer mouse). The participants were instructed  
394 to fixate on the centre of the screen and remain still for the duration of each block (3 blocks of approximately 11  
395 minutes each, with a few minutes break between blocks). A grey background was presented onscreen where faces  
396 appeared one at a time. Stimuli were presented using the Cogent 2000 toolbox for MATLAB  
397 (<http://www.vislab.ucl.ac.uk/cogent.php>). Each face was displayed for 200ms to minimise the likelihood of  
398 saccades. Whenever the face was not on the screen, a cross was displayed to help participants maintain central  
399 fixation. The next trial did not begin until after the participant responded using the button box to indicate whether  
400 the face was male or female. Left/right assignment for male/female did not change across the three blocks but the  
401 assignment was counterbalanced between participants. Participants were required to make their response as  
402 accurately and as quickly as they could. The inter-trial interval (ITI) was jittered between 750 and 1,500ms to  
403 reduce onset predictability.

### 404 **Stimuli**

405 The face stimuli originated from the Karolinksa Directed Emotional Faces set (KDEF; Lundqvist, Flykt, &  
406 Ohman, 1998). Image dimensions were 198 x 252 pixels and all images were greyscale. Spatial frequency was  
407 manipulated by applying a low-pass cut-off of  $<6$  cycles/image to create the Low spatial frequency stimuli and  
408 by applying a high-pass cut-off of  $>24$  cycles/image to create the High spatial frequency stimuli (**Fig. 1**). Broad  
409 spatial frequency stimuli were images with no altered frequency information. Luminance and contrast of the Low

410 and High spatial frequency images was matched to their respective Broad spatial frequency image by using the  
411 SHINE toolbox for MATLAB<sup>67</sup>. There were 60 identities: 30 males and 30 females. Each identity was presented  
412 once per condition (3 spatial frequency levels x 2 emotional expressions) resulting in six presentations per block.  
413 Hence, the three blocks resulted in a total of 180 trials per condition. All faces were presented in a random order  
414 per block but the same identity was never sequentially presented. A photodiode was placed at the bottom-left  
415 corner of the screen to record precise stimulus onset.

## 416 **MEG Data Acquisition**

417 Neural activity was recorded using a whole-head 306-sensor (102 magnetometers and 102 pairs of orthogonally  
418 oriented planar gradiometers) Elekta Neuromag TRIUX system (Elekta Neuromag Oy, Helsinki, Finland).  
419 Activity was recorded at a sampling rate of 1,000 Hz. Before entering the MEG room, head position indicator  
420 (HPI) coils were positioned on each participant (three on the forehead and one behind each ear). An  
421 electromagnetic digitizer system was used to determine the location of the coils relative to anatomical fiducials at  
422 the nasion and at the left and right preauricular points (FastTrak, Polhemus, Colchester, VT, USA).  
423 Electrooculographic (EOG) electrodes were also placed above and below the right eye to record eye blinks. When  
424 seated in the scanner, participants were positioned so that the helmet of the MEG was in as much contact with the  
425 head as comfortably possible. Total scanning time was 30-40 minutes, including breaks. Head position was  
426 tracked continuously using the HPI coils.

## 427 **MEG Preprocessing**

428 The temporal extension of Signal-Space Separation (tSSS; Taulu & Simola, 2006) was applied using the MaxFilter  
429 software (Elekta Neuromag, Helsinki, Finland), actively cancelling noise and interpolating bad channels. The  
430 MaxMove function was also used to correct for head movement using a standard reference head position (0x, 0y,  
431 40z). All subsequent offline preprocessing was completed using SPM12 (Wellcome Trust Centre for  
432 Neuroimaging, University College London, UK) via MATLAB 2014a (The Mathworks Inc., Natwick, MA, USA).  
433 The data were down-sampled to 200Hz and a band-pass filter of 0.5 – 30Hz was applied. Each participant's MEG  
434 data were coregistered with their anatomical T1 MRI image, which was acquired at the same site (Swinburne  
435 University of Technology, Melbourne, Australia) immediately after completing the MEG scan.

436 Due to a technical error, EOG activity for the first four participants was not recorded. Thus, for blink correction,  
437 a frontal MEG planar gradiometer (channel MEG0922) was substituted as the EOG, given its proximity to the  
438 upper EOG sensor and the presence of the eyeblink artefact in the signal. Eyeblink artefacts were identified as a  
439 3fT/mm deviation in the EOG signal and then marking a -300 to 300ms time window around this deviation. The  
440 associated sensor topographies were used to correct the MEG data.

441 For analysis, the MEG data were segmented into -100 to 650ms blocks of planar gradiometer activity time-locked  
442 to stimulus onset and baseline-corrected, creating a series of event-related fields (ERFs). For the spatiotemporal  
443 analysis, the ERF for each trial was converted to 3D scalp/time images (*x* space, *y* space, *ms* time) and then  
444 smoothed with an 8mm x 8mm x 20ms FWHM Gaussian kernel to accommodate for intersubject variability. For  
445 dynamic causal modelling, ERFs were averaged using the robust averaging function in SPM12, which weights  
446 the contribution of an epoch to the average based on its relative noise<sup>68</sup>. A low-pass filter of 30Hz and baseline  
447 correction were re-applied to the averaged ERFs to account for any high-frequency noise introduced by robust  
448 averaging.

## 449 **Dynamic Causal Modelling**

450 Dynamic causal modelling (DCM) was used to compare different plausible neural networks that may underlie the  
451 observed neural data. DCM is a biologically-informed computational method of estimating the effective  
452 connectivity between brain regions using Bayesian statistics<sup>69</sup>. We constructed several anatomical models that  
453 were based closely on previous work by Garvert et al.<sup>14</sup> who also investigated neural networks of emotional face  
454 perception. These anatomical models (**Fig. 4**) included the lateral geniculate nucleus (LGN; MNI coordinates: left  
455 = -22 -22 -6, right = 22 -22 -6) and pulvinar (PUL; MNI coordinates: left = -12 -25 7, right = 12 -25 7), each  
456 receiving visual sensory input, and the primary visual cortex (V1; MNI coordinates: left = -7 -85 -7, right = 7 -85  
457 -7) and amygdala (AMY; MNI coordinates: left = -23 -5 -22, right = 23 -5 -22). All models encompassed only the

458 first 300ms (i.e. 0-300ms post-stimulus onset) of the ERFs, as we were interested primarily in the earliest stages  
459 of visual processing.

460 Bayesian model estimation (via the expectation maximisation algorithm) and random-effects Bayesian model  
461 selection (which compromises between explanatory power and model complexity and accounts for variability  
462 across participants) was used to determine the most likely anatomical model for our data<sup>70</sup>. This was followed by  
463 a series of functional models for how these connections were modulated by either spatial frequency, emotion, or  
464 both (**Fig. 5**). Finally, sensitivity analysis was conducted to investigate the contribution of each parameter – either  
465 by an incremental change in an anatomical connection or by the specific modulations of spatial frequency or  
466 emotion (**Fig. 6**).

## 467 **References**

- 468 1. Mobbs, D., Hagan, C. C., Dalgleish, T., Silston, B. & Prévost, C. The ecology of human fear: Survival  
469 optimization and the nervous system. *Front. Neurosci.* **9**, 1–22 (2015).
- 470 2. Murray, R. J., Brosch, T. & Sander, D. The functional profile of the human amygdala in affective  
471 processing: Insights from intracranial recordings. *Cortex* **60**, 10–33 (2014).
- 472 3. Morris, J. S., Ohman, a & Dolan, R. J. A subcortical pathway to the right amygdala mediating ‘unseen’  
473 fear. *Proc. Natl. Acad. Sci. U. S. A.* **96**, 1680–1685 (1999).
- 474 4. LeDoux, J. *The emotional brain: The mysterious underpinnings of emotional life.* (Simon and Schuster,  
475 1998).
- 476 5. Pessoa, L. & Adolphs, R. Emotion and the brain: multiple roads are better than one. *Nat. Rev. Neurosci.*  
477 **12**, 425 (2011).
- 478 6. Pessoa, L. & Adolphs, R. Emotion processing and the amygdala: from a ‘low road’ to ‘many roads’ of  
479 evaluating biological significance. *Nat. Rev. Neurosci.* **11**, 773–783 (2010).
- 480 7. de Gelder, B., van Honk, J. & Tamietto, M. Emotion in the brain: of low roads, high roads and roads less  
481 travelled. *Nat. Rev. Neurosci.* **12**, 425; author reply 425 (2011).
- 482 8. Cauchoix, M. & Crouzet, S. M. How plausible is a subcortical account of rapid visual recognition? *Front.*  
483 *Hum. Neurosci.* **7**, 1–4 (2013).
- 484 9. Furl, N., Henson, R. N., Friston, K. J. & Calder, A. J. Top-Down Control of Visual Responses to Fear by  
485 the Amygdala. *J. Neurosci.* **33**, 17435–17443 (2013).
- 486 10. Morris, J. S. *et al.* A neuromodulatory role for the human amygdala in processing emotional facial  
487 expressions. *Brain* **121** ( Pt 1, 47–57 (1998).
- 488 11. Tamietto, M. & de Gelder, B. Neural bases of the non-conscious perception of emotional signals. *Nat.*  
489 *Rev. Neurosci.* **11**, 697–709 (2010).
- 490 12. Rafal, R. D. *et al.* Connectivity between the superior colliculus and the amygdala in humans and macaque  
491 monkeys: virtual dissection with probabilistic DTI tractography. *J. Neurophysiol.* **114**, 1947–62 (2015).
- 492 13. Tamietto, M., Pullens, P., De Gelder, B., Weiskrantz, L. & Goebel, R. Subcortical connections to human  
493 amygdala and changes following destruction of the visual cortex. *Curr. Biol.* **22**, 1449–1455 (2012).
- 494 14. Garvert, M. M., Friston, K. J., Dolan, R. J. & Garrido, M. I. Subcortical amygdala pathways enable rapid  
495 face processing. *Neuroimage* **102**, 309–316 (2014).
- 496 15. Rudrauf, D. *et al.* Rapid Interactions between the Ventral Visual Stream and Emotion-Related Structures  
497 Rely on a Two-Pathway Architecture. *J. Neurosci.* **28**, 2793–2803 (2008).
- 498 16. Berman, R. a & Wurtz, R. H. Functional identification of a pulvinar path from superior colliculus to  
499 cortical area MT. *J. Neurosci.* **30**, 6342–6354 (2010).
- 500 17. Day-Brown, J. D., Wei, H., Chomsung, R. D., Petry, H. M. & Bickford, M. E. Pulvinar projections to the  
501 striatum and amygdala in the tree shrew. *Front. Neuroanat.* **4**, 143 (2010).



- 502 18. Silverstein, D. N. & Ingvar, M. A multi-pathway hypothesis for human visual fear signaling. *Front. Syst.*  
503 *Neurosci.* **9**, 1–20 (2015).
- 504 19. Öhman, A. The role of the amygdala in human fear: Automatic detection of threat.  
505 *Psychoneuroendocrinology* **30**, 953–958 (2005).
- 506 20. Vuilleumier, P., Armony, J. L., Driver, J. & Dolan, R. J. Distinct spatial frequency sensitivities for  
507 processing faces and emotional expressions. *Nat. Neurosci.* **6**, 624–631 (2003).
- 508 21. Mendez-Bertolo, C. *et al.* A fast pathway for fear in human amygdala. *Nat. Neurosci.* (2016).  
509 doi:10.1038/nn.4324
- 510 22. Zhang, P., Zhou, H., Wen, W. & He, S. Layer-specific response properties of the human lateral geniculate  
511 nucleus and superior colliculus. *Neuroimage* **111**, 159–66 (2015).
- 512 23. Kastner, S. *et al.* Functional Imaging of the Human Lateral Geniculate Nucleus and Pulvinar. *J*  
513 *Neurophysiol* **17**, 17 (2003).
- 514 24. Le, Q. Van *et al.* Snakes elicit earlier, and monkey faces, later, gamma oscillations in macaque pulvinar  
515 neurons. *Sci. Rep.* **6**, 20595 (2016).
- 516 25. Nguyen, M. N. *et al.* Neuronal responses to face-like stimuli in the monkey pulvinar. *Eur. J. Neurosci.*  
517 **37**, 35–51 (2013).
- 518 26. De Cesarei, A. & Codispoti, M. Spatial frequencies and emotional perception. *Rev. Neurosci.* **24**, 89–104  
519 (2013).
- 520 27. David, O. *et al.* Dynamic causal modeling of evoked responses in EEG and MEG. *Neuroimage* **30**, 1255–  
521 1272 (2006).
- 522 28. Pourtois, G., Dan, E. S., Grandjean, D., Sander, D. & Vuilleumier, P. Enhanced extrastriate visual  
523 response to bandpass spatial frequency filtered fearful faces: Time course and topographic evoked-  
524 potentials mapping. *Hum. Brain Mapp.* **26**, 65–79 (2005).
- 525 29. Schyns, P. G. & Oliva, A. Dr. Angry and Mr. Smile: when categorization flexibly modifies the perception  
526 of faces in rapid visual presentations. *Cognition* **69**, 243–265 (1999).
- 527 30. Deruelle, C. & Fagot, J. Categorizing facial identities, emotions, and genders: Attention to high- and low-  
528 spatial frequencies by children and adults. *J. Exp. Child Psychol.* **90**, 172–184 (2005).
- 529 31. Goffaux, V., Jemel, B., Jacques, C., Rossion, B. & Schyns, P. G. ERP evidence for task modulations on  
530 face perceptual processing at different spatial scales. *Cogn. Sci.* **27**, 313–325 (2003).
- 531 32. Aguado, L., Serrano-Pedraza, I., Rodríguez, S. & Román, F. J. Effects of spatial frequency content on  
532 classification of face gender and expression. *Span. J. Psychol.* **13**, 525–37 (2010).
- 533 33. Winston, J. S., Vuilleumier, P. & Dolan, R. J. Effects of Low-Spatial Frequency Components of Fearful  
534 Faces on Fusiform Cortex Activity. *Curr. Biol.* **13**, 1824–1829 (2003).
- 535 34. Awasthi, B., Sowman, P. F., Friedman, J. & Williams, M. A. Distinct spatial scale sensitivities for early  
536 categorization of faces and places: neuromagnetic and behavioral findings. *Front. Hum. Neurosci.* **7**, 91  
537 (2013).
- 538 35. Vlamings, P. H. J. M., Goffaux, V. & Kemner, C. Is the early modulation of brain activity by fearful facial  
539 expressions primarily mediated by coarse low spatial frequency information? *J. Vis.* **9**, 12–12 (2009).
- 540 36. Peyrin, C. *et al.* The neural substrates and timing of top-down processes during coarse-to-fine  
541 categorization of visual scenes: a combined fMRI and ERP study. *J. Cogn. Neurosci.* **22**, 2768–2780  
542 (2010).
- 543 37. Craddock, M., Martinovic, J. & Müller, M. M. Task and Spatial Frequency Modulations of Object  
544 Processing : An EEG Study. *PLoS One* **8**, 1–12 (2013).
- 545 38. Mu, T. & Li, S. The neural signature of spatial frequency-based information integration in scene  
546 perception. *Exp. Brain Res.* **227**, 367–377 (2013).
- 547 39. Vuilleumier, P. How brains beware: Neural mechanisms of emotional attention. *Trends Cogn. Sci.* **9**, 585–

- 548 594 (2005).
- 549 40. Garrido, M. I., Kilner, J. M., Kiebel, S. J. & Friston, K. J. Evoked brain responses are generated by  
550 feedback loops. *Proc. Natl. Acad. Sci. U. S. A.* **104**, 20961–20966 (2007).
- 551 41. Garrido, M. I. *et al.* Repetition suppression and plasticity in the human brain. *Neuroimage* **48**, 269–279  
552 (2009).
- 553 42. FitzGerald, T. H. B., Moran, R. J., Friston, K. J. & Dolan, R. J. Precision and neuronal dynamics in the  
554 human posterior parietal cortex during evidence accumulation. *Neuroimage* **107**, 219–228 (2015).
- 555 43. Dietz, M. J., Friston, K. J., Mattingley, J. B., Roepstorff, A. & Garrido, M. I. Effective connectivity reveals  
556 right-hemisphere dominance in audiospatial perception: implications for models of spatial neglect. *J.*  
557 *Neurosci.* **34**, 5003–11 (2014).
- 558 44. Daunizeau, J., Kiebel, S. J. & Friston, K. J. Dynamic causal modelling of distributed electromagnetic  
559 responses. *Neuroimage* **47**, 590–601 (2009).
- 560 45. Mermillod, M., Bonin, P., Mondillon, L., Alleysson, D. & Vermeulen, N. Coarse scales are sufficient for  
561 efficient categorization of emotional facial expressions: Evidence from neural computation.  
562 *Neurocomputing* **73**, 2522–2531 (2010).
- 563 46. de Gelder, B., Hortensius, R. & Tamietto, M. Attention and awareness each influence amygdala activity  
564 for dynamic bodily expressions—a short review. *Front. Integr. Neurosci.* **6**, 54 (2012).
- 565 47. Bridge, H., Leopold, D. A. & Bourne, J. A. Adaptive Pulvinar Circuitry Supports Visual Cognition.  
566 *Trends Cogn. Sci.* **20**, 146–157 (2016).
- 567 48. Hedger, N., Gray, K. L. H., Garner, M. & Adams, W. J. Are Visual Threats Prioritized Without  
568 Awareness? A Critical Review and Meta-Analysis Involving 3 Behavioral Paradigms and 2696  
569 Observers. *Psychol. Bull.* (2016). doi:10.1037/bul0000054
- 570 49. Johnson, M. H. Subcortical face processing. *Nat. Rev. Neurosci.* **6**, 766–774 (2005).
- 571 50. Willenbockel, V., Lepore, F., Nguyen, D. K., Bouthillier, A. & Gosselin, F. Spatial frequency tuning  
572 during the conscious and non-conscious perception of emotional facial expressions - An intracranial ERP  
573 study. *Front. Psychol.* **3**, 1–12 (2012).
- 574 51. Attal, Y., Maess, B., Friederici, A. & David, O. Head models and dynamic causal modeling of subcortical  
575 activity using magnetoencephalographic/electroencephalographic data. *Rev. Neurosci.* **23**, 85–95 (2012).
- 576 52. Dumas, T. *et al.* MEG Evidence for Dynamic Amygdala Modulations by Gaze and Facial Emotions. *PLoS*  
577 *One* **8**, 1–11 (2013).
- 578 53. Garrido, M. I., Barnes, G. R., Sahani, M. & Dolan, R. J. Functional evidence for a dual route to amygdala.  
579 *Curr. Biol.* **22**, 129–134 (2012).
- 580 54. Krolak-salmon, P. *et al.* Early Amygdala Reaction to Fear Spreading in Occipital, Temporal, and Frontal  
581 Cortex: A Depth Electrode ERP Study in Human. **42**, 665–676 (2004).
- 582 55. Liddell, B. J. *et al.* A direct brainstem-amygdala-cortical ‘alarm’ system for subliminal signals of fear.  
583 *Neuroimage* **24**, 235–243 (2005).
- 584 56. Maior, R. S., Hori, E., Tomaz, C., Ono, T. & Nishijo, H. The monkey pulvinar neurons differentially  
585 respond to emotional expressions of human faces. *Behav. Brain Res.* **215**, 129–135 (2010).
- 586 57. Almeida, I., Soares, S. C. & Castelo-Branco, M. The distinct role of the amygdala, superior colliculus and  
587 pulvinar in processing of central and peripheral snakes. *PLoS One* **10**, 1–21 (2015).
- 588 58. Van Le, Q. *et al.* Pulvinar neurons reveal neurobiological evidence of past selection for rapid detection of  
589 snakes. *Proc. Natl. Acad. Sci.* **110**, 19000–19005 (2013).
- 590 59. Stein, T., Seymour, K., Hebart, M. N. & Sterzer, P. Rapid fear detection relies on high spatial frequencies.  
591 *Psychol. Sci.* **25**, 566–574 (2014).
- 592 60. Fradcourt, B., Peyrin, C., Baciú, M. & Campagne, A. Behavioral assessment of emotional and  
593 motivational appraisal during visual processing of emotional scenes depending on spatial frequencies.

- 594 *Brain Cogn.* **83**, 104–113 (2013).
- 595 61. de Gardelle, V. & Kouider, S. How Spatial Frequencies and Visual Awareness Interact During Face  
596 Processing. *Psychol. Sci.* **21**, 58–66 (2010).
- 597 62. Ruiz-Soler, M. & Beltran, F. S. Face perception: An integrative review of the role of spatial frequencies.  
598 *Psychol. Res.* **70**, 273–292 (2006).
- 599 63. Sowden, P. T. & Schyns, P. G. Channel surfing in the visual brain. *Trends Cogn. Sci.* **10**, 538–545 (2006).
- 600 64. Sander, D., Grafman, J. & Zalla, T. The Human Amygdala: An Evolved System for Relevance Detection.  
601 *Rev. Neurosci.* 303–316 (2003).
- 602 65. Carr, J. A. I'll take the low road: the evolutionary underpinnings of visually triggered fear. *Front.*  
603 *Neurosci.* **9**, 1–13 (2015).
- 604 66. Nomi, J. S. & Uddin, L. Q. Face processing in autism spectrum disorders: From brain regions to brain  
605 networks. *Neuropsychologia* **71**, 201–216 (2015).
- 606 67. Willenbockel, V. *et al.* Controlling low-level image properties: the SHINE toolbox. *Behav Res Methods*  
607 **42**, 671–684 (2010).
- 608 68. Litvak, V. *et al.* EEG and MEG data analysis in SPM8. *Comput. Intell. Neurosci.* **2011**, (2011).
- 609 69. Daunizeau, J., David, O. & Stephan, K. E. Dynamic causal modelling: A critical review of the biophysical  
610 and statistical foundations. *Neuroimage* **58**, 312–322 (2011).
- 611 70. Stephan, K. E., Penny, W. D., Daunizeau, J., Moran, R. J. & Friston, K. J. Bayesian model selection for  
612 group studies. *Neuroimage* **46**, 1004–1017 (2009).
- 613